

Full-counting statistics of energy transport of molecular junctions in the polaronic regime

Gaomin Tang,¹ Zhizhou Yu,¹ and Jian Wang^{1,*}

¹*Department of Physics and the Center of Theoretical and Computational Physics, The University of Hong Kong, Hong Kong, China and The University of Hong Kong Shenzhen Institute of Research and Innovation, Shenzhen, China*

(Dated: June 18, 2019)

We investigate the full-counting statistics (FCS) of energy transport carried by electrons in molecular junctions for the Anderson-Holstein model in the polaronic regime. Using two-time quantum measurement scheme, generating function (GF) for the energy transport is derived and expressed as a Fredholm determinant in terms of Keldysh nonequilibrium Green's function in the time domain. Dressed tunneling approximation is used in decoupling the phonon cloud operator in the polaronic regime. This formalism facilitates us to analyze the time evolution of energy transport dynamics after a sudden switch-on of the coupling between the dot and the leads towards the stationary state. Transient dynamics of energy current cumulants is numerically calculated and analyzed. The universal scaling of normalized transient energy cumulants is found under the external bias. The steady state energy current cumulant GF in the long time limit is obtained in the energy domain as well. Universal relations for steady state energy current FCS is derived under finite temperature gradient with zero bias and this enables us to express the equilibrium energy current cumulant by a linear combination of lower order cumulants. Behaviors of energy current cumulants under temperature gradient and external bias are numerically shown and explained.

PACS numbers: 73.23.-b, 05.40.Ca, 05.60.Gg, 44.05.+e

I. INTRODUCTION

Rapid experimental development in the field of nanotechnology facilitates us to fabricate the single-molecule junctions^{1,2}, of which the goal is to extend the lifetime of Moore's law. The charging of the molecule leads to elastic mechanical deformations, and hence causes an interaction between electronic and the quantized mechanical degrees of freedom, which is the electron-phonon coupling. Molecular junctions in which a strong electron-phonon coupling can lead to polaronic regime^{3,4} could reveal to us a variety of intriguing transport properties, such as phonon-assisted current steps and Franck-Condon blockade⁵. Such a junction could be modeled as a quantum dot described by the Anderson-Holstein model^{6,7} coupled to two electrodes.

Efforts have been made both on theoretical and computational methods, such as master equations^{8–11}, diagrammatic quantum Monte Carlo¹², and numerical renormalization group¹³, on transport problems involving electron-phonon interactions. However, lots of numerical calculations are involved in these methodologies. Nonequilibrium Green's function (NEGF) technique is a powerful tool to deal with a wide range of physical problems of nonequilibrium systems and in principle the most appropriate method to study interaction effects in the time-dependent properties. In order to decouple the phonon cloud operator in the polaronic regime, dressed tunneling approximation (DTA), in which the leads' self-energies are dressed with the polaronic cloud, has been proposed to eliminate the noticeable pathological features of the single particle approximation at low frequencies and polaron tunneling approximation at high frequencies^{14–16}.

Quantum transport is in nature a stochastic process and a physical quantity of a stochastic process could be characterized by the corresponding distribution function¹⁷. Full-counting statistics (FCS) which was initiated by Levitov and Lesovik^{18–20} could give us a full scenery of probability distribution of electron and energy transport^{15,16,21–30}. The key in FCS is to obtain the generating function (GF) which is actually the Fourier transform of probability distribution of related physical quantity. Using the NEGF technique^{31–34} and path integral method under the two-time quantum measurement scheme^{23,35–37}, GF is formulated as a Fredholm determinant in the time domain both in the phonon^{25–27} and electron^{23,28–30} transport systems. This formalism enables us to study transient regime which could help us have a better understanding in the short time dynamics²⁸. Transient dynamics of particle current transport in the molecular junctions in the polaronic regime has been reported by Souto *et al.*¹⁶.

The transport study of energy flow in the nonequilibrium system could reveal us the information on how energy is dissipated and its correlation for electronic devices and can be investigated theoretically by Landauer-Büttiker type of formalism for noninteracting systems^{38–40}. Energy transport in trapped ion chains has been measured experimentally in the work by M. Ramm *et al.*⁴¹. The heat current I_α^h in the α lead could be related to the energy current I_α^E by the expression $I_\alpha^h = I_\alpha^E - \mu_\alpha I_\alpha$ with the particle current I_α and the chemical potential μ_α in the α lead, and this quantity is quite important in characterizing the efficiency of thermoelectric devices⁴². So far, FCS of energy transfer mostly focuses on phonon transport both in the transient regime and steady states^{25–27} and less attention has been

paid to the FCS of energy transfer carried by electrons in the electronic transport problems. In our previous work, we investigated the transient FCS of energy transfer in the non-interacting system³⁰. It would be important and interesting as well to study of FCS of energy transport carried by electrons of molecular junctions in the polaronic regime under both transient dynamics and steady state, and this is the purpose of this work.

In the present work, FCS of energy transport carried by electrons in molecular junctions for the Anderson-Holstein model in the polaronic regime is investigated both in the transient regime and steady state. In terms of NEGF under DTA, GF for the energy current is derived from the equation of motion and could be expressed as a Fredholm determinant in the time domain. Numerical calculation is performed and allows us to analyze the time evolution of the system towards the steady state which undergoes an external bias after a sudden switch-on of the coupling between the dot and the leads. The energy current cumulant GF for the in the steady state is obtained in the energy domain as well and universal relations for energy current cumulants under finite temperature gradient with zero bias. We also calculate and analyze the various order cumulants (from the first to the fourth) under temperature gradient or external bias.

The rest of the article is organized as follows. In Sec. II, the model Hamiltonian of a molecular junction is introduced and GF of energy flow in the transient regime is given in terms of NEGF in the time domain. In Sec. III, transient dynamics of energy current is investigated under and external bias. Sec. IV is devoted to the steady state investigation of energy current, both theoretically and numerically. Finally, a brief conclusion is drawn in Sec. V.

II. MODEL AND BASIC THEORETICAL FORMALISM

Only considering the lowest electronic orbital, the single-molecule is simplified as a single electronic level of a quantum dot (QD) being coupled to localized vibrational mode, which is the simplest spinless Anderson-Holstein model. The QD then is coupled to the left and right electrode so that the system will undergo a nonequilibrium state when the external bias or temperature gradient is applied (Fig. 1). The corresponding Hamiltonian reads as

$$H = H_S + H_L + H_R + H_T \quad (1)$$

with the Hamiltonian of the central dot (in natural units, $\hbar = k_B = e = m_e = 1$)

$$H_S = \epsilon_0 d^\dagger d + \omega_0 a^\dagger a + t_{ep}(a^\dagger + a)d^\dagger d, \quad (2)$$

where ϵ_0 is the bare electronic energy level, and ω_0 is the frequency of the localized vibron. d^\dagger (a^\dagger) denotes the

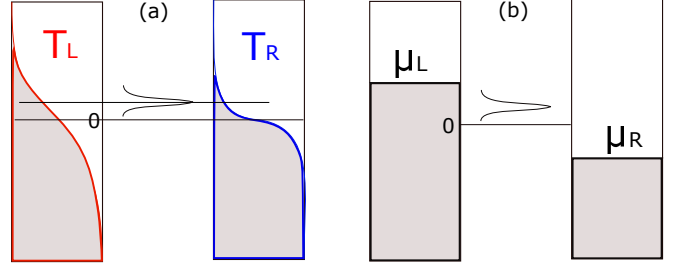


FIG. 1. Sketch of a QD coupled the left and right lead under (a) temperature gradient $T_L > T_R$ with zero chemical potentials in both leads and (b) external bias $\Delta\mu$ with $\mu_{L(R)} = \pm \Delta\mu/2$ under zero temperature.

electron (phonon) creation operator in the QD. The localized vibron modulates the QD with the electron-phonon coupling constant t_{ep} . The Hamiltonians of the leads are

$$H_\alpha = \sum_{x \in k\alpha} \epsilon_x c_x^\dagger c_x, \quad (3)$$

where the indices $k\alpha = kL, kR$ are used to label the different states in the left and right leads. H_T is the Hamiltonian describing the coupling between the dot and the leads with the tunneling amplitudes $t_{k\alpha}$,

$$H_T = H_{LS} + H_{RS} = \sum_{k\alpha} (t_{k\alpha} c_{k\alpha}^\dagger d + t_{k\alpha}^* d^\dagger c_{k\alpha}). \quad (4)$$

The tunneling rate (linewidth function) of lead α is assumed to bear the Lorentzian form and could be expressed as

$$\Gamma_\alpha(\omega) = \text{Im} \sum_k \frac{|t_{k\alpha}|^2}{\omega - \epsilon_{k\alpha} - i0^+} = \frac{\Gamma_\alpha W^2}{\omega^2 + W^2}, \quad (5)$$

with the linewidth amplitude Γ_α and bandwidth W , and one can denote $\Gamma = \Gamma_L + \Gamma_R$.

The electron-vibron coupling term can be eliminated by applying the Lang-Firsov unitary transformation⁴³ given by

$$\bar{H} = S H S^\dagger, \quad S = e^{g d^\dagger d (a^\dagger - a)}, \quad g = \frac{t_{ep}}{\omega_0}, \quad (6)$$

which leads to

$$\bar{H}_S = \bar{\epsilon} d^\dagger d + \omega_0 a^\dagger a, \quad (7)$$

where the bare QD electron energy is changed to $\bar{\epsilon} = \epsilon_0 - g^2 \omega_0$. The tunneling Hamiltonian is transformed as

$$\bar{H}_T = \sum_{k\alpha} (t_{k\alpha} c_{k\alpha}^\dagger X d + t_{k\alpha}^* d^\dagger X^\dagger c_{k\alpha}) \quad (8)$$

with the phonon cloud operator $X = \exp[g(a - a^\dagger)]$, while Hamiltonian of the uncoupled leads remains unchanged.

In the present work we study the transient dynamics in which the interaction between the leads and the QD

is suddenly turned on at $t = 0$ and afterwards the system evolves to the steady states. The turning on process could be accessed by a quantum point contact which is controlled by a gate voltage. The initial density matrix of the whole system at $t = 0$ is the direct product of each subsystem and expressed by $\rho(0) = \rho_L \otimes \rho_S \otimes \rho_R$. The statistical behaviors of the energy current in a specific lead are all encoded in the probability distribution $P(\Delta\epsilon, t)$ of the transferred energy carried by electrons $\Delta\epsilon = \epsilon_t - \epsilon_0$ between an initial time $t = 0$ and a later time t . The GF $Z(\lambda, t)$ with the counting field λ is defined as,

$$Z(\lambda, t) \equiv \langle e^{i\lambda\Delta\epsilon} \rangle = \int P(\Delta\epsilon, t) e^{i\lambda\Delta\epsilon} d\Delta\epsilon. \quad (9)$$

The j th cumulant of transferred energy $\langle\langle(\Delta\epsilon)^j\rangle\rangle$ could be calculated by taking the j th derivative of cumulant generating function (CGF) which is $\ln Z(\lambda)$ with respect to $i\lambda$,

$$C_k(t) \equiv \langle\langle(\Delta\epsilon)^k\rangle\rangle = \left. \frac{\partial^k \ln Z(\lambda)}{\partial(i\lambda)^k} \right|_{\lambda=0}. \quad (10)$$

One can further define the energy current cumulants

$$\langle\langle(I^E)^k\rangle\rangle = \frac{\partial C_k(t)}{\partial t}, \quad (11)$$

which tend to the steady state energy current cumulants in the long time limit $t \rightarrow \infty$.

To investigate statistical behaviors of the energy current through the left lead, we could focus on the energy operator which is actually the free Hamiltonian of the left lead H_L . Under the two-time measurement scheme, GF of transferred energy in the left lead can be expressed over the Keldysh contour as^{23,27,29},

$$\begin{aligned} Z(\lambda, t) &= \text{Tr} \left\{ \rho(0) \mathcal{T}_C \exp \left[-\frac{i}{\hbar} \int_C H_\gamma(t') dt' \right] \right\} \\ &= \text{Tr} \left\{ \rho(0) U_{\lambda/2}^\dagger(t, 0) U_{-\lambda/2}(t, 0) \right\}, \end{aligned} \quad (12)$$

with the modified evolution operator ($\gamma = \pm\lambda/2$ depending on the branch of the contour),

$$U_\gamma(t, 0) = \mathcal{T} \exp \left[-\frac{i}{\hbar} \int_0^t H_\gamma(t') dt' \right]. \quad (13)$$

Here the modified evolution operator is expressed by the modified Hamiltonian,

$$\begin{aligned} H_\gamma &= \bar{H}_S + \sum_k \left[\epsilon_{kL} c_{kL}^\dagger(t_\gamma) c_{kL}(t_\gamma) + \epsilon_{kR} c_{kR}^\dagger c_{kR} \right] \\ &+ \sum_k \left[\left(t_{kL} c_{kL}^\dagger(t_\gamma) X d + t_{kR} c_{kR}^\dagger X d \right) + \text{H.c.} \right], \end{aligned} \quad (14)$$

with $t_\gamma = \hbar\gamma$, and $c_{kL}(t_\gamma) = e^{i\gamma H_L} c_{kL}(0) e^{-i\gamma H_L}$.

GF for the transferred charges in transient regime has been expressed by NEGF in the time domain for the

non-interacting case²⁹ and polaronic regime using the DTA^{15,16}. GF for the energy current has expressed by NEGF and higher-order cumulants has been investigated by Z. Yu *et al.* for the non-interacting case³⁰. We now generalize the GF for the energy current to the interacting case in the polaronic regime following the derivation of the GF for transferred charges¹⁶. Starting from the derivative of the Eq. (12) with respect to the counting field,

$$\begin{aligned} \frac{\partial Z}{\partial \lambda} &= \int_C dt' \sum_k \left\langle \mathcal{T}_C \left(t_{kL} c_{kL}^\dagger(t' \mp \hbar\lambda/2) X(t') d(t') \right. \right. \\ &\quad \left. \left. - t_{kL}^* d^\dagger(t') X^\dagger(t') c_{kL}(t' \pm \hbar\lambda/2) \right) \right\rangle, \end{aligned} \quad (15)$$

where we take ' $-$ ' in the first part and ' $+$ ' in the second for the forward time contour, while inversely for the backward contour. The equation of motion of the three point Green function on the contour $\langle\langle \mathcal{T}_C c_{kL}^\dagger(t') X(t) d(t_2) \rangle\rangle$ is

$$\begin{aligned} &\left(i \frac{\partial}{\partial t'} - \epsilon_{kL} \right) \langle\langle \mathcal{T}_C c_{kL}^\dagger(t') X(t) d(t_2) \rangle\rangle \\ &= t_{kL}^* \langle\langle \mathcal{T}_C d^\dagger(t') X^\dagger(t') X(t) d(t_2) \rangle\rangle \end{aligned} \quad (16)$$

which could be written in an integral form³²

$$\begin{aligned} &\langle\langle \mathcal{T}_C c_{kL}^\dagger(t') X(t) d(t_2) \rangle\rangle \\ &= \int_C dt_1 \langle\langle \mathcal{T}_C d^\dagger(t_1) X^\dagger(t_1) X(t) d(t_2) \rangle\rangle t_{kL}^* g_{kL}(t_1, t') \end{aligned} \quad (17)$$

Under DTA, one has the decoupling¹⁶

$$\begin{aligned} &\langle\langle \mathcal{T}_C d^\dagger(t_1) X^\dagger(t_1) X(t) d(t_2) \rangle\rangle \\ &\simeq \langle\langle \mathcal{T}_C X^\dagger(t_1) X(t) \rangle\rangle \langle\langle \mathcal{T}_C d^\dagger(t_1) d(t_2) \rangle\rangle = \Lambda(t, t_1) G(t_2, t_1), \end{aligned} \quad (18)$$

with $\Lambda(t, t_1) = \langle\langle \mathcal{T}_C X^\dagger(t_1) X(t) \rangle\rangle$ being the phonon cloud propagator of which the form will be discussed later. Then we have

$$t_{kL} \langle\langle \mathcal{T}_C c_{kL}^\dagger(t') X(t') d(t') \rangle\rangle = \int_C dt_1 G(t', t_1) \Lambda(t', t_1) \Sigma(t_1, t'). \quad (19)$$

The self-energies due to the coupling to the leads under the DTA could be expressed as,

$$\Sigma_{\alpha, D}^{ab}(t_1, t_2) = \Sigma_\alpha^{ab}(t_1, t_2) \Lambda^{ba}(t_2, t_1) = \Sigma_\alpha^{ab}(t_1, t_2) \Lambda^{ab}(t_1, t_2), \quad (20)$$

where $a, b = +, -$ denote different Keldysh components and

$$\Sigma_\alpha^{ab}(t_1, t_2) = ab \theta(t_1) \theta(t_2) \sum_k t_{k\alpha}^* g_{k\alpha}^{ab}(t_1, t_2) t_{k\alpha}. \quad (21)$$

The counting field enters the self-energy in absence of the phonon cloud operator and the modified self-energy can

be expressed by $\tilde{\Sigma}_L^{ab}(t_1, t_2) = \Sigma_L^{ab}(t_1 - t_2 - (a - b)\hbar\lambda)$. One can rewrite Eq. (15) as

$$\frac{\partial Z}{\partial \lambda} = - \int_0^t dt_1 \int_0^t dt_2 \text{Tr}_K \left\{ \frac{\partial \tilde{\Sigma}_{L,D}(t_1, t_2)}{\partial \lambda} G(t_2, t_1) \right\}, \quad (22)$$

Tr_K indicates the trace is over the Keldysh space. GF could be expressed in the Fredholm determinant by the Keldysh NEGF in the time domain as¹⁶,

$$Z(\lambda, t) = \det \left(G \tilde{G}^{-1} \right) \quad (23)$$

with

$$\begin{aligned} G^{-1} &= G_0^{-1} - \Sigma_{L,D} - \Sigma_{R,D}, \\ \tilde{G}^{-1} &= G_0^{-1} - \tilde{\Sigma}_{L,D} - \Sigma_{R,D}, \end{aligned} \quad (24)$$

where G_0 denotes the Green's function of the uncoupled QD, and the *tilde* indicates the inclusion of the counting field in the self-energy $\Sigma_{\alpha,D}$. The Green's functions and self-energies without counting field possess the Keldysh structure,

$$A = \begin{pmatrix} A^{++} & A^{+-} \\ A^{-+} & A^{--} \end{pmatrix}. \quad (25)$$

The phonon cloud operator $\Lambda^{ab}(t_1, t_2)$ is given by⁷,

$$\Lambda^{+-}(t_1, t_2) = [\Lambda^{-+}(t_1, t_2)]^* = \sum_{m=-\infty}^{\infty} \alpha_m e^{im\omega_0(t_1-t_2)}, \quad (26)$$

with

$$\alpha_m = e^{-g^2(2n_B+1)} e^{m\beta\omega_0/2} I_m \left(2g^2 \sqrt{n_B(1+n_B)} \right), \quad (27)$$

I_m being the modified Bessel function of the first kind, and Bose factor $n_B = 1/(e^{\beta\omega_0} - 1)$, $\beta = 1/k_B T$. $T = T_{L(R)}$ is the temperature of the lead where the phonon cloud operator couples, this would be important in the system with a temperature gradient. At zero-temperature α_m could be simplified as,

$$\alpha_m = \begin{cases} e^{-g^2} g^{2m}/m! & \text{if } m \geq 0 \\ 0 & \text{if } m < 0 \end{cases}. \quad (28)$$

The remaining components could be calculated by the relations,

$$\begin{aligned} \Lambda^{++}(t_1, t_2) &= \theta(t_1 - t_2) \Lambda^{-+}(t_1, t_2) + \theta(t_2 - t_1) \Lambda^{+-}(t_1, t_2), \\ \Lambda^{--}(t_1, t_2) &= \theta(t_2 - t_1) \Lambda^{-+}(t_1, t_2) + \theta(t_1 - t_2) \Lambda^{+-}(t_1, t_2). \end{aligned} \quad (29)$$

The Dyson equation bearing a Keldysh structure under DTA is

$$G = G_0 + G_0 \Sigma_D G. \quad (30)$$

where $\Sigma_D = \Sigma_{L,D} + \Sigma_{R,D}$.

Utilizing the Dyson equation, Eq. (23) could be written as,

$$Z(\lambda, t) = \det \left[I - G \left(\tilde{\Sigma}_{L,D} - \Sigma_{L,D} \right) \right]. \quad (31)$$

so that CGF has the form,

$$\ln Z(\lambda, t) = \text{Tr} \ln \left[I - G \left(\tilde{\Sigma}_{L,D} - \Sigma_{L,D} \right) \right], \quad (32)$$

by using the relation $\det B = \exp[\text{Tr} \ln B]$. Taking the first order derivative of GF and noting that $\tilde{\Sigma}_L^{+-}(t_1, t_2) = -\sum_k t_{kL}^* g_{kL}^{+-}(t_1 - t_2 - \lambda) t_{kL}$, energy current in the transient regime can be expressed as,

$$I_L^E(t) = \int dt' \left[G^{+-}(t, t') \check{\Sigma}^{-+}(t', t) - G^{-+}(t, t') \check{\Sigma}^{+-}(t', t) \right], \quad (33)$$

where

$$\check{\Sigma}^{+-}(t', t) = -\Lambda^{+-}(t' - t) \sum_k \epsilon_{kL} t_{kL}^* g_{kL}^{+-}(t' - t) t_{kL}. \quad (34)$$

and similarly for $\check{\Sigma}^{-+}(t', t)$. The transient current expression agrees with the one which was obtained directly by NEGF method⁴⁴.

III. TRANSIENT DYNAMICS OF ENERGY TRANSPORT

In order to investigate the very short time behaviors, to the lowest order in the time domain, we have the expansion of the GF,

$$Z(\lambda, t) \approx 1 + \int_0^t dt_1 \int_0^t dt_2 \left[\tilde{\Sigma}_{L,D}^{-+}(t_1, t_2) - \Sigma_{L,D}^{-+}(t_1, t_2) \right] G_0^{+-}(t_2, t_1) + \left[\tilde{\Sigma}_{L,D}^{+-}(t_1, t_2) - \Sigma_{L,D}^{+-}(t_1, t_2) \right] G_0^{-+}(t_2, t_1) \quad (35)$$

The expressions for uncoupled dot Green's function and self-energy are presented in Appendix. Under wide-band limit $W \rightarrow \infty$, we can obtain the GF in the short time limit with a close-packed form as,

$$Z(\lambda, t) \approx 1 + A_{L0}(n_d - 1) + A_{L1}n_d, \quad (36)$$

where

$$\begin{aligned} A_{L0} &= \frac{\Gamma_L}{\pi} \sum_{n=-\infty}^{\infty} \alpha_n \int d\omega (e^{i\omega\lambda} - 1) M(\omega) f_{L+n}(\omega), \\ A_{L1} &= \frac{\Gamma_L}{\pi} \sum_{n=-\infty}^{\infty} \alpha_n \int d\omega (e^{-i\omega\lambda} - 1) M(\omega) [f_{L-n}(\omega) - 1]. \end{aligned} \quad (37)$$

with

$$M(\omega) = \frac{1 - \cos[(\omega - \bar{\epsilon})t]}{(\omega - \bar{\epsilon})^2}. \quad (38)$$

Here and below $f_{\alpha\pm n}$ is shorthand for $f_{\alpha}(\omega \pm n\omega_0)$. We can see from the short time limit expression of the GF that the transport process is unidirectional in the short time limit.

We apply the formalism to perform numerical calculation with respect to the transient dynamics of energy current under external bias, respectively. The energies are measured in the unit of Γ and $1/\Gamma$ is the unit of time. We only consider the case where the QD is initially unoccupied $n_d = 0$ and the linewidth amplitude in Eq. (5) is set to be $\Gamma_L = \Gamma_R = \Gamma/2$ and the bandwidth is also set to be the same for both leads with $W = 10\Gamma$.

First to fourth transient energy current cumulants, $\langle\langle(I^E)^k\rangle\rangle$ for $k = 1, 2, 3, 4$, in the left lead for increasing g under external bias are shown in Fig. 2. Increasing g corresponds to the increasing of the electron-phonon coupling strength. The frequency of the localized vibron $\omega_0 = 6\Gamma$. The renormalized energy level of the QD is $\bar{\epsilon} = 1.5\Gamma$. The chemical potential of the left and right lead are chosen to be $\mu_L = 2\Gamma$ and $\mu_R = -2\Gamma$.

As a general feature for both the non-interacting ($g = 0$) and interacting cases, the transient amplitudes of $\langle\langle(I^E)^k\rangle\rangle$ increase with cumulants order. This behavior is universal and will be investigated in detail in Fig. 3. The second and fourth energy current cumulants may even oscillate to negative values in the short times. The amplitudes of oscillation in the evolution and the asymptotic values of the cumulants are suppressed with the increasing of g . The first and third energy current cumulants in the stationary limit are positive, since we put the normalized energy level of QD above the Fermi energy of the both leads so that the electrons with positive energy mainly contribute to the transport process. However, in short times, the energy current and third cumulant oscillate to negative values with a minimum. Since the QD is prepared initially empty, once the system is connected, the electron mainly from the left lead will contribute to the transport process which could be seen from Eq. (36),

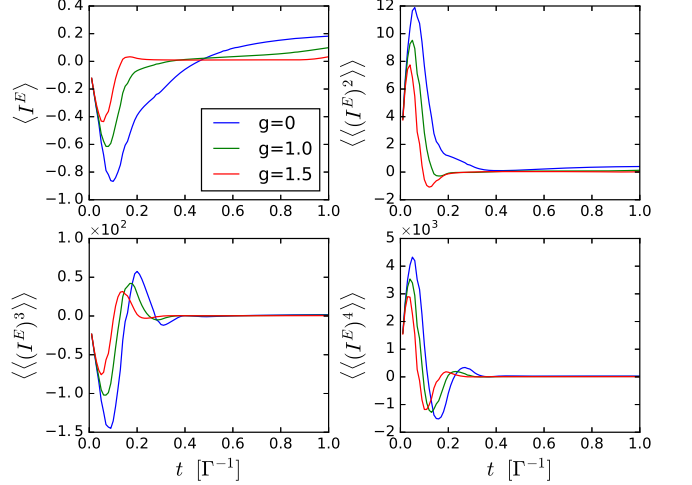


FIG. 2. 1st to 4th transient energy current cumulants in the left lead for increasing g (0 (blue), 1.0 (green) and 1.5 (red)) for initially empty QD under external bias at zero temperature. The energies are measured in the unit of Γ and $1/\Gamma$ is the unit of time. The chemical potential of the left and right lead are chosen to be $\mu_{L(R)} = \pm 2\Gamma$. The renormalized energy level of the QD is $\bar{\epsilon} = 1.5\Gamma$ and the frequency of the localized vibron $\omega_0 = 6\Gamma$.

so that negative energy far below the Fermi energy in the left lead will mainly contribute to the energy transport process.

We also plot the logarithm of maximum amplitude of the normalized transient energy cumulants $M_k = \max|C_k/C_1|$ in Fig. (3). Different lines with respect to different bandwidths W are plotted, while the other parameters are same as in Fig. 2. Maximum amplitudes M_k for different interaction parameter $g = 0, 1.0$ and 1.5 coincide. We can see from the figure that both $\ln(M_{2k})$ and $\ln(M_{2k+1})$ are linear with cumulants order k with the slope close to 3 but they have different intercepts. This universal scaling of normalized transient energy cumulants is the result of the universality of the GF in the short time which was also reported in the charge cumulants^{16,45}. Analytic explanation for the noninteracting case under external bias was reported in our previous work³⁰.

IV. STEADY STATE ENERGY TRANSPORT FCS

In the long-time limit, the system goes to steady state, and the Dyson equation Eq. (30) bearing the Keldysh structure in the energy domain could be expressed by

$$G = G_0 + G_0 \Sigma_D G, \quad (39)$$

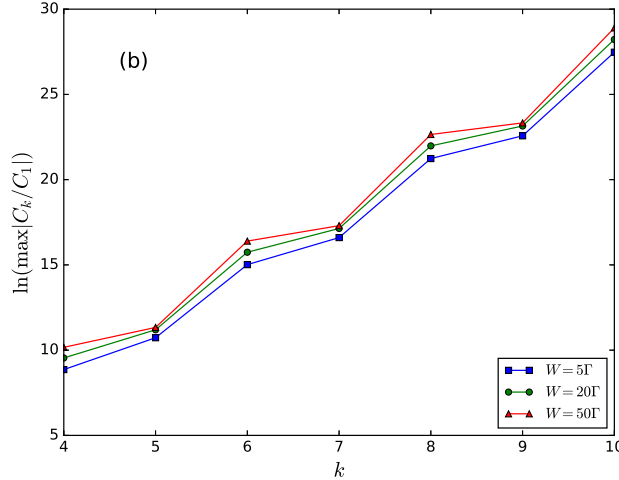


FIG. 3. Logarithm of maximum amplitude of the normalized transient energy cumulants $M_k = \max|C_k/C_1|$ at short times versus k for different bandwidths W under external bias. Maximum amplitudes M_k for different interaction parameters $g = 0, 1.0$ and 1.5 coincide.

so that¹⁵

$$G = \frac{-1}{\mathcal{D}(\omega)} \begin{bmatrix} -(\omega - \bar{\epsilon}) - \Sigma_D^{--} & -\Sigma_D^{+-} \\ -\Sigma_D^{-+} & (\omega - \bar{\epsilon}) - \Sigma_D^{++} \end{bmatrix}, \quad (40)$$

with

$$\mathcal{D}(\omega) = [\omega - \bar{\epsilon} - \Sigma_D^r(\omega)][\omega - \bar{\epsilon} - \Sigma_D^a(\omega)]. \quad (41)$$

The dressed retarded self-energy in frequency domain could be obtained by the Fourier transformation of the time domain counterpart with the form $\Sigma_D^r(t_1, t_2) = \theta(t_1 - t_2) [\Sigma_D^{+-}(t_1, t_2) - \Sigma_D^{-+}(t_1, t_2)]$, so that in wide band limit $W \rightarrow \infty$ (WBL),¹⁵

$$\Sigma_{\alpha, D}^r(\omega) = \sum_m \alpha_m \int \frac{dE}{2\pi} \frac{\Gamma_\alpha [1 + f_{\alpha+m}(E) - f_{\alpha-m}(E)]}{\omega - E + i0^+}. \quad (42)$$

The real and imaginary part could be obtained using Plemelj formula $1/(E \pm i0^+) = P(1/E) \mp i\pi\delta(E)$ which will facilitate the numerical calculation as well. One can verify that the real part and imaginary part satisfies

$$\begin{aligned} \text{Im} [\Sigma_{\alpha, D}^r(\mu_\alpha + \omega)] &= \text{Im} [\Sigma_{\alpha, D}^r(\mu_\alpha - \omega)], \\ \text{Re} [\Sigma_{\alpha, D}^r(\mu_\alpha + \omega)] &= -\text{Re} [\Sigma_{\alpha, D}^r(\mu_\alpha - \omega)], \end{aligned} \quad (43)$$

respectively¹⁵.

In the long-time limit, the Green's function and self-energy in Eq. (32) become time translation invariant so that scaled cumulant generating function (SCGF) $\mathcal{F}(\lambda) = \lim_{t \rightarrow \infty} \ln Z(\lambda)/t$ could be expressed in the en-

ergy domain as

$$\begin{aligned} \mathcal{F}(\lambda) = \int \frac{d\omega}{2\pi} \ln & \left\{ 1 + \sum_{mn} T_{mn}(\omega) [f_{L+m}(1 - f_{R-n}) \right. \\ & \left. \times (e^{i\lambda\omega} - 1) + f_{R+n}(1 - f_{L-m})(e^{-i\lambda\omega} - 1)] \right\}. \end{aligned} \quad (44)$$

In this expression $T_{mn}(\omega)$ is the transmission coefficient involving m and n vibrational quanta in the left and right lead, respectively, with the form,

$$T_{mn}(\omega) = \frac{\Gamma_L \Gamma_R \alpha_m \alpha_n}{\mathcal{D}(\omega)}. \quad (45)$$

Now we consider the universal relations for energy current cumulants under finite temperature gradient with zero bias which is in analogy with the universal relation for particle current cumulants^{46,47}. Using the relation $\alpha_{-m} = e^{-\beta_L m \omega_0} \alpha_m$, $\alpha_{-n} = e^{-\beta_R n \omega_0} \alpha_n$ and $f_R(1 - f_L) = \exp(\Delta\beta\omega) f_L(1 - f_R)$ with $\Delta\beta = \beta_L - \beta_R$ for $\Delta\mu = 0$ in Eq. (44), we have the symmetry relation

$$\mathcal{F}(\xi) = \mathcal{F}(-\xi + \Delta\beta) \quad (46)$$

with $i\lambda$ being replaced by ξ for convenience. In the linear response regime $\Delta\beta \rightarrow 0$, we can expand both sides as Taylor series around $\Delta\beta = 0$ and $\xi = 0$, which could lead to,

$$\frac{\partial^k \mathcal{F}(-\xi + \Delta\beta)}{\partial \Delta\beta^k} \Big|_0 = \sum_{l=0}^k \binom{k}{l} \frac{\partial^k \mathcal{F}(\xi)}{\partial \Delta\beta^{k-l} \partial \xi^l} \Big|_0. \quad (47)$$

Since $\mathcal{F}(\xi = 0) = 0$, the above equality equals to zero as well. The last term in the summation of Eq. (47) is the k th derivative of the GF with respect to the counting field ξ , which is actually $\langle\langle (I^E)^k \rangle\rangle$ at equilibrium. Then we have the relation

$$\langle\langle (I^E)^k \rangle\rangle = - \sum_{l=1}^{k-1} \binom{k}{l} \frac{\partial^{k-l} \langle\langle (I^E)^l \rangle\rangle}{\partial \Delta\beta^{k-l}}, \quad (48)$$

in which the energy current cumulant at equilibrium is expressed by a linear combination of lower order energy current cumulants.

We now show numerical calculations regarding steady state energy current cumulants under temperature gradient and external bias of molecular junctions in the polaronic regime. The energies are measured in the unit of vibron frequency ω_0 , and the linewidth amplitude is chosen to be $\Gamma = 0.05\omega_0$ which indicates weak coupling. WBL is taken in our steady state calculation.

The first to fourth energy current cumulants for increasing g versus temperature gradient $\Delta T = T_L - T_R$ with the left lead warmer and temperature of right lead fixed at $k_B T_R = 0.2\omega_0$ are shown in Fig. (4). The chemical potentials in both leads are set to be zero and the renormalized energy level of the QD is $\bar{\epsilon} = 0$. The energy

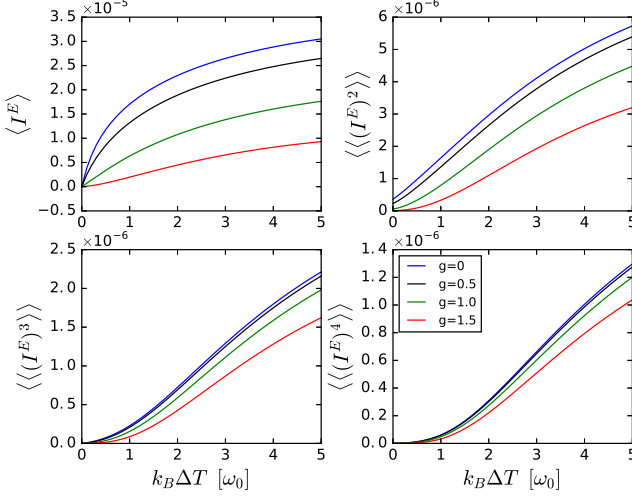


FIG. 4. 1st to 4th energy current cumulants for increasing g (0 (blue), 0.5 (green), 1.0 (black) and 1.5 (red)) versus temperature gradient $\Delta T = T_L - T_R$ with the left lead warmer and temperature of right lead fixed at $k_B T_R = 0.2\omega_0$. The renormalized energy level of the QD is $\bar{\epsilon} = 0$.

current cumulants become smaller with the increasing of g because of the suppression of transport due to electron-phonon interaction. The second energy current cumulant with zero temperature gradient is finite due to the thermal noise in the leads, and it is reduced with increasing g .

In Fig. (5), energy current cumulants with different renormalized energy levels of the QD with $g = 1$ are plotted. We can see that the first to fourth cumulants and SCGF as well are even functions of $\bar{\epsilon}$. Since the chemical potentials of both leads are zero, one can let

$$X_{mn}(\omega) = f_{L+m}(\omega)[1 - f_{R-n}(\omega)]e^{i\lambda\omega} + f_{R+n}(\omega)[1 - f_{L-m}(\omega)]e^{-i\lambda\omega}, \quad (49)$$

and verify that,

$$X_{mn}(\omega) = X_{mn}(-\omega), \quad (50)$$

using the relation $f_{L+m}(\omega) = 1 - f_{L-m}(-\omega)$. In WBL, from Eq. (43), the real and imaginary part of the dressed retarded self-energy is the odd and even function of ω , respectively, so that we have the following symmetry with respect to the transmission coefficient in the polaronic regime

$$T_{mn}(\omega, \bar{\epsilon}) = T_{mn}(-\omega, -\bar{\epsilon}). \quad (51)$$

where the dependency of $\bar{\epsilon}$ has been written explicitly. Then, we have the following symmetry of SCGF with respect to $\bar{\epsilon}$,

$$\mathcal{F}(\lambda, \bar{\epsilon}) = \mathcal{F}(\lambda, -\bar{\epsilon}). \quad (52)$$

with $\mu_L = \mu_R = 0$ in WBL. One can see from Fig. (5), $\langle I^E \rangle(\bar{\epsilon} = 2\omega_0)$ is smaller than $\langle I^E \rangle(\bar{\epsilon} = \omega_0)$ under small

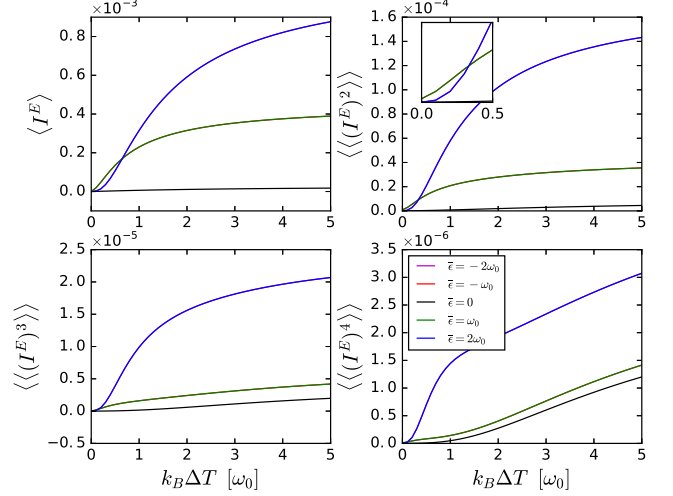


FIG. 5. 1st to 4th energy current cumulants for different renormalized energy levels of the QD $\bar{\epsilon}$ ($-2\omega_0$ (magenta), $-\omega_0$ (red), 0 (black) ω_0 (green) and $2\omega_0$ (blue)) versus temperature gradient $\Delta T = T_L - T_R$ with $k_B T_R = 0.2\omega_0$. $g = 1.0$. 1st to 4th cumulants are even functions of $\bar{\epsilon}$.

temperature gradient, because the number of electrons for transport in the left lead is smaller at $\bar{\epsilon} = 2\omega_0$ than at $\bar{\epsilon} = \omega_0$. This is also for the second energy current cumulant. The energy near $\bar{\epsilon}$ mainly contributes to the transport process. When T_L increases, $f_L(\omega) - f_R(\omega)$ near $\omega = 2\omega_0$ could exceed the one near $\omega = \omega_0$, so that the first and second cumulant with larger $\bar{\epsilon}$ is larger than the ones with smaller $\bar{\epsilon}$.

The first to fourth energy current cumulants for increasing g versus external bias $\Delta\mu$ with $\mu_L = \Delta\mu/2$ and $\mu_R = -\Delta\mu/2$ are shown in Fig. (6). Temperatures of both leads are chosen to be very small with $k_B T_L = k_B T_R = 0.04\omega_0$. The renormalized energy level of the QD is $\bar{\epsilon} = 2\omega_0$. For the non-interacting case, the energy current and second cumulant are almost zero below the bias $\Delta\mu = 4\omega_0 = 2\bar{\epsilon}$ and experience a platform when the external bias exceeds $2\bar{\epsilon}$. This is because when $\Delta\mu = 2\bar{\epsilon}$, chemical potential of the left lead is equal to the renormalized energy of QD, $\mu_L = \bar{\epsilon}$, in which energy the transmission coefficient is in its largest value. Electron-phonon coupling enables the step size to become smaller, however creates smaller steps at $\Delta\mu = 2\bar{\epsilon} + 2n\omega_0$ with $n = 1, 2, 3 \dots$. This is due to the presence of sidebands in the leads.

The third and fourth energy current cumulants have a dip at $\Delta\mu = 2\bar{\epsilon}$ with fourth cumulant larger for both non-interacting and interacting cases. Polaronic regime creates smaller dips at $\Delta\mu = 2\bar{\epsilon} + 2n\omega_0$ with $n = 1, 2, 3 \dots$ which could also be identified in Fig. (8). Increasing g reduces the amplitude of the dip at $\Delta\mu = 2\bar{\epsilon}$ but increases the amplitude at $\Delta\mu = 2\bar{\epsilon} + 2n\omega_0$. For the non-interacting

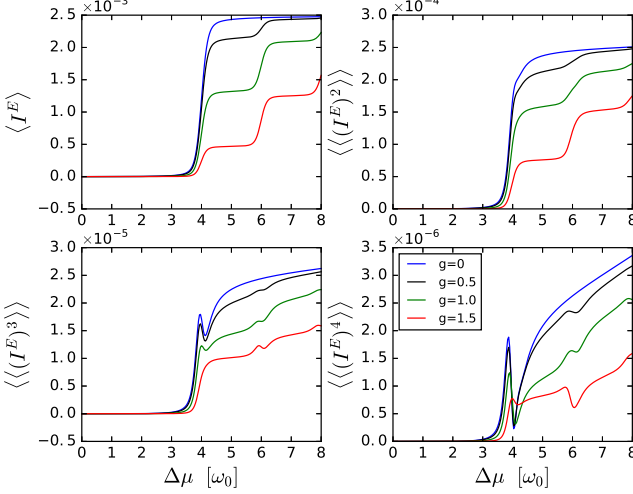


FIG. 6. 1st to 4th energy current cumulants for increasing g (0 (blue), 0.5 (green), 1.0 (black) and 1.5 (red)) versus external bias $\Delta\mu$ with $\mu_L = \Delta\mu/2$ and $\mu_R = -\Delta\mu/2$. Temperatures of both leads are $k_B T_L = k_B T_R = 0.04\omega_0$. The renormalized energy level of the QD is chosen to be $\bar{\epsilon} = 2\omega_0$.

case under zero-temperature, one can get,

$$\begin{aligned} \langle I^E \rangle &= \int \frac{d\omega}{2\pi} \omega T(\omega), \\ \langle\langle\langle I^E \rangle^2 \rangle\rangle &= \int \frac{d\omega}{2\pi} \omega^2 T(\omega) [1 - T(\omega)], \\ \langle\langle\langle I^E \rangle^3 \rangle\rangle &= \int \frac{d\omega}{2\pi} \omega^3 T(\omega) [1 - T(\omega)] [1 - 2T(\omega)], \\ \langle\langle\langle I^E \rangle^4 \rangle\rangle &= \int \frac{d\omega}{2\pi} \omega^4 T(\omega) [1 - T(\omega)] [1 - 6T(\omega) + 6T^2(\omega)]. \end{aligned} \quad (53)$$

with the ranges of integration from $-\Delta\mu/2$ to $\Delta\mu/2$ omitted for succinctness. We can further take derivative of $\langle\langle\langle I^E \rangle^k \rangle\rangle$ with respect to external bias $\Delta\mu$, $\partial\langle I^E \rangle / \partial\Delta\mu$ and $\partial\langle\langle\langle I^E \rangle^2 \rangle\rangle / \partial\Delta\mu$ is always positive since the transmission coefficient for non-interacting case has the form $T(\omega) = \frac{\Gamma^2/4}{(\omega - \bar{\epsilon})^2 + \Gamma^2/4}$. However the derivative of the third and fourth cumulant with respect to external bias change sign around $\Delta\mu = 2\bar{\epsilon}$ which leads to the presence of the dips in Fig. (6).

The influence of temperature on cumulants under external bias is reported in Fig. (7), one can see that both the steps and dips get smoothed or even disappear when temperature increases.

In Fig. (8), energy current cumulants with different $\bar{\epsilon}$ with $g = 1$ are plotted. We can see that the first and third cumulants are odd functions of $\bar{\epsilon}$, while the second and fourth cumulants are even functions of $\bar{\epsilon}$. The reason is as follows, under zero temperature, the transport is unidirectional and Fermi-Dirac distribution function $f_{L(R)}$ has a step-wise form, since $\mu_R = -\mu_L$, the energies of electrons which mainly contribute to the transport corresponding to $\bar{\epsilon}$ has a different sign with the energies

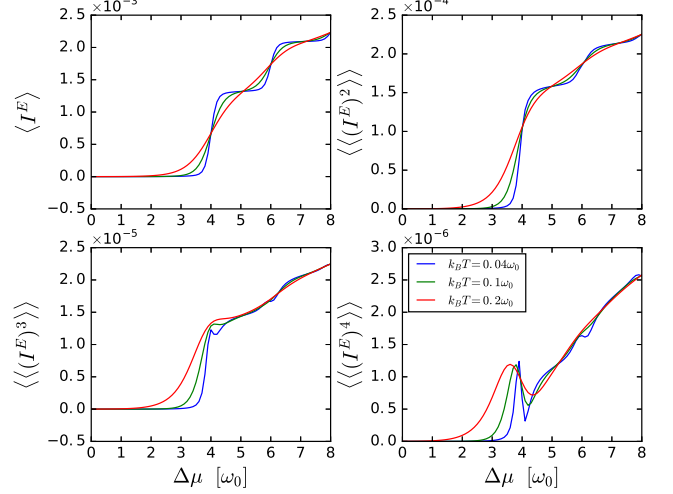


FIG. 7. 1st to 4th energy current cumulants for increasing temperatures $k_B T$ ($0.04\omega_0$ (blue), $0.1\omega_0$ (green) and $0.2\omega_0$ (red)) versus external bias $\Delta\mu$ with $\mu_{L(R)} = \pm\Delta\mu/2$. $g = 1.0$ and $\bar{\epsilon} = 2\omega_0$.

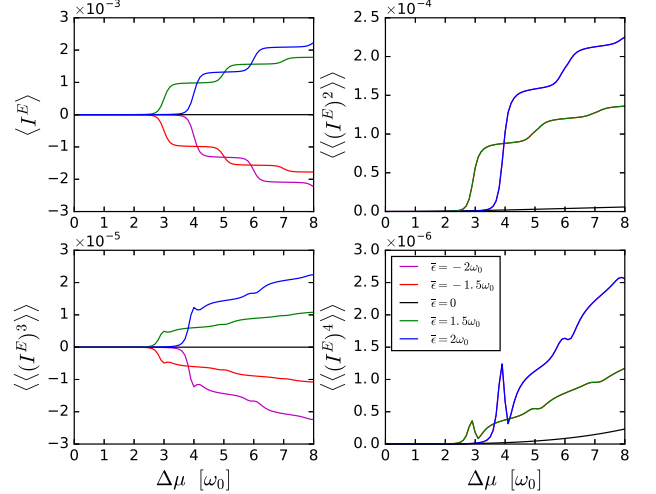


FIG. 8. 1st to 4th energy current cumulants for different $\bar{\epsilon}$ ($-2\omega_0$ (magenta), $-1.5\omega_0$ (red), 0 (black) $1.5\omega_0$ (green) and $2\omega_0$ (blue)) versus external bias $\Delta\mu$ with $\mu_L = \Delta\mu/2$ and $\mu_R = -\Delta\mu/2$. $g = 1.0$ and temperatures of both leads are $k_B T_L = k_B T_R = 0.04\omega_0$.

corresponding to $-\bar{\epsilon}$.

V. CONCLUSION

Both transient and steady state behaviors of energy transport carried by electrons in molecular junctions for the Anderson-Holstein model in the polaronic regime have been investigated using FCS. Using two-time measurement scheme and equation of motion technique, GF

for the energy current could be expressed as a Fredholm determinant in the time domain using NEGF. The DTA decoupling scheme¹⁴ which could provide a good description in dealing with the phonon cloud operator has been adapted in obtaining GF. This formalism facilitates us to analyze the time evolution of energy transport dynamics after a sudden switch of the coupling between the dot and the leads towards the stationary state. The amplitudes of oscillation in the evolution and the asymptotic values of the cumulants are suppressed with the increasing of g . The universal scaling of normalized transient energy cumulants is found under external bias.

Universal relations for energy current cumulants under finite temperature gradient with zero bias and this enables us to express the equilibrium energy current cumulant by a linear combination of lower order cumulants. Behaviors of energy current cumulants (from the first to the fourth) under temperature gradient and external bias are numerically shown and explained.

ACKNOWLEDGMENTS

This work was financially supported by the Research Grant Council (Grant No. HKU 705212P), the University Grant Council (Contract No. AoE/P-04/08) of the Government of HKSAR, NSF-China under Grant No. 11374246.

APPENDIX: GREEN'S FUNCTION AND THE SELF-ENERGY IN THE TIME DOMAIN

Description on how to calculate the uncoupled dot Green's function and the self-energy in the time domain in the absence of the phonon cloud operator is sketched here. The four correlation functions of the uncoupled dot

are given in the book by A. Kamenev,³⁴

$$\begin{aligned} iG_0^{+-}(t_1, t_2) &= -n_d \exp\{-i\bar{\epsilon}(t_1 - t_2)\} \\ iG_0^{-+}(t_1, t_2) &= (1 - n_d) \exp\{-i\bar{\epsilon}(t_1 - t_2)\} \\ iG_0^{++}(t_1, t_2) &= \theta(t_1 - t_2) iG_0^{-+} + \theta(t_2 - t_1) iG_0^{+-} \\ iG_0^{--}(t_1, t_2) &= \theta(t_2 - t_1) iG_0^{-+} + \theta(t_1 - t_2) iG_0^{+-}, \end{aligned} \quad (54)$$

where n_d is the initial occupation number of the QD before the system is connected. Lorentzian linewidth function with the linewidth amplitude Γ_α and band width W ,

$$\Gamma_\alpha(\omega) = \frac{\Gamma_\alpha W^2}{\omega^2 + W^2}, \quad (55)$$

is used to describe the self-energy $\Sigma_{L(R)}$ in absence of the phonon cloud operator, so that the numerical calculation would be more realistic. The equilibrium energy dependent self-energy can be written as,

$$\Sigma_\alpha^r(\omega) = \frac{\Gamma_\alpha W}{2(\omega + iW)}. \quad (56)$$

Performing Fourier transform, the retarded self-energy in the time domain could be obtained,²⁹

$$\Sigma_\alpha^r(t_1, t_2) = -\frac{i}{2} \theta(t_1 - t_2) \Gamma_\alpha W e^{-(i\mu_\alpha + W)(t_1 - t_2)}, \quad (57)$$

where μ_α is the chemical potential of the α -lead. For the lesser self-energy in the time domain,

$$\Sigma_\alpha^<(t_1, t_2) = i \int \frac{d\omega}{2\pi} e^{-i\omega(t_1 - t_2)} f_\alpha(\omega) \Gamma_L(\omega - \mu_\alpha) \quad (58)$$

with $f_\alpha(\omega) = 1 / [e^{\beta(\omega - \mu_\alpha)} + 1]$. It is a function of the time difference, and one can let $\tau = t_1 - t_2$ for convenience. When $t_1 = t_2$,

$$\Sigma_\alpha^<(t_1, t_2) = \frac{i}{4} \Gamma_\alpha W. \quad (59)$$

The case of $t_1 > t_2$ for both the zero and non-zero temperature is to be considered first. At non-zero temperature, if $t_1 > t_2$, it has poles $\frac{-i(2n+1)\pi}{\beta_\alpha}$ and $-iW$, where $n = 0, 1, 2, 3, \dots$, so that,

$$\begin{aligned} \Sigma_\alpha^<(t_1, t_2) &= \frac{i\Gamma_\alpha W}{2} e^{-i\mu_\alpha \tau} \left\{ e^{-W\tau} \left[1 + \frac{E1(-W\tau)}{2i\pi} \right] - e^{W\tau} \frac{E1(W\tau)}{2i\pi} \right\} \quad k_B T_\alpha = 0, \\ \Sigma_\alpha^<(t_1, t_2) &= \frac{i\Gamma_\alpha W}{2} e^{-i\mu_\alpha \tau} \left\{ \frac{\exp(-W\tau)}{\exp(-i\beta_\alpha W) + 1} - \frac{2}{i\beta_\alpha} \sum_{n=0}^{+\infty} \exp\left[-\frac{(2n+1)\pi}{\beta_\alpha}\tau\right] \frac{W}{W^2 - \left[\frac{(2n+1)\pi}{\beta_\alpha}\right]^2} \right\} \quad k_B T_\alpha \neq 0, \end{aligned} \quad (60)$$

where $E1(x) = \int_x^\infty \frac{e^{-t}}{t} dt$. Using the relation $\Sigma_\alpha^<(t_1, t_2)|_{t_1 < t_2} = -[\Sigma_\alpha^<(t_1, t_2)|_{t_1 > t_2}]^*$, the full expres-

sion of $\Sigma_\alpha^<(t_1, t_2)$ could be obtained. The remaining com-

ponents could be calculated by the relations,

$$\begin{aligned}\Sigma_{\alpha}^{>}(t_1, t_2) &= \Sigma_{\alpha}^{<}(t_1, t_2) + \Sigma_{\alpha}^r(t_1, t_2) - \Sigma_{\alpha}^a(t_1, t_2), \\ \Sigma_{\alpha}^t(t_1, t_2) &= \theta(t_1 - t_2)\Sigma_{\alpha}^{>}(t_1 - t_2) + \theta(t_2 - t_1)\Sigma_{\alpha}^{<}(t_1 - t_2), \\ \Sigma_{\alpha}^{\bar{t}}(t_1, t_2) &= \theta(t_2 - t_1)\Sigma_{\alpha}^{>}(t_1 - t_2) + \theta(t_1 - t_2)\Sigma_{\alpha}^{<}(t_1 - t_2).\end{aligned}\quad (61)$$

We point out here $\Sigma_{\alpha}^{++} = \Sigma_{\alpha}^t$, $\Sigma_{\alpha}^{+-} = -\Sigma_{\alpha}^{<}$, $\Sigma_{\alpha}^{-+} = -\Sigma_{\alpha}^{>}$, and $\Sigma_{\alpha}^{--} = \Sigma_{\alpha}^{\bar{t}}$.

* jianwang@hku.hk

- ¹ J. Reichert, R. Ochs, D. Beckmann, H. B. Weber, M. Mayor, and H. v. Löhneysen, Phys. Rev. Lett. **88**, 176804 (2002).
- ² W. Liang, M. Shores, M. Bockrath, J. Long, and H. Park, Nature **417**, 725 (2002).
- ³ F. Ortmann, F. Bechstedt, and K. Hannewald, Phys. Rev. B **79**, 235206 (2009).
- ⁴ F. Ortmann and S. Roche, Phys. Rev. B **84**, 180302 (2011).
- ⁵ J. Koch, F. von Oppen, and A. V. Andreev, Phys. Rev. B **74**, 205438 (2006).
- ⁶ T. Holstein, Ann. Phys. (NY) **8**, 343 (1959).
- ⁷ G. D. Mahan, *Many-Particle Physics*, 3rd ed. (Kluwer Academic, 2000).
- ⁸ J. Koch and F. von Oppen, Phys. Rev. Lett. **94**, 206804 (2005).
- ⁹ J. Koch, M. E. Raikh, and F. von Oppen, Phys. Rev. Lett. **95**, 056801 (2005).
- ¹⁰ A. Zazunov, D. Feinberg, and T. Martin, Phys. Rev. B **73**, 115405 (2006).
- ¹¹ X. Y. Shen, B. Dong, X. L. Lei, and N. J. M. Horing, Phys. Rev. B **76**, 115308 (2007).
- ¹² L. Mühlbacher and E. Rabani, Phys. Rev. Lett. **100**, 176403 (2008).
- ¹³ A. Jovchev and F. B. Anders, Phys. Rev. B **87**, 195112 (2013).
- ¹⁴ R. Seoane Souto, A. Levy Yeyati, A. Martn-Rodero, and R. C. Monreal, Phys. Rev. B **89**, 085412 (2014).
- ¹⁵ B. Dong, G. H. Ding, and X. L. Lei, Phys. Rev. B **88**, 075414 (2013).
- ¹⁶ R. S. Souto, R. Avriller, R. C. Monreal, A. Martn-Rodero, and A. L. Yeyati, Phys. Rev. B **92**, 125435 (2015).
- ¹⁷ Ya. Blanter, and M. Büttiker, Phys. Rep. **336**, 1 (2000).
- ¹⁸ L. S. Levitov, and G. B. Lesovik, Pisma Zh. Eksp. Teor. Fiz. **58**, 225 (1993) [Sov. Phys.JETP **58**, 230 (1993)].
- ¹⁹ L. S. Levitov, H.-W. Lee, and G. B. Lesovik, J. Math. Phys. **37**, 4845 (1996).
- ²⁰ L. S. Levitov, in *Quantum Noise in Mesoscopic Physics, NATO Science Series II*, Vol. 97, edited by Yu. V. Nazarov (Kluwer, Dordrecht, 2003).
- ²¹ I. Klich, in *Quantum Noise in Mesoscopic Physics, NATO Science Series II*, Vol. 97, edited by Yu. V. Nazarov (Kluwer, Dordrecht, 2003).
- ²² Yu. V. Nazarov, and M. Kindermann, Eur. Phys. J. B **35**, 413-420 (2003).
- ²³ M. Esposito, U. Harbola and S. Mukamel, Rev. Mod. Phys. **81**, 1665 (2009).
- ²⁴ F. Hassler, M. V. Suslov, G. M. Graf, M. V. Lebedev, G. B. Lesovik, and G. Blatter, Phys. Rev. B **78**, 165330 (2008).
- ²⁵ J.-S. Wang, B. K. Agarwalla, and H. Li, Phys. Rev. B **84**, 153412 (2011).
- ²⁶ B. K. Agarwalla, B. Li, and J.-S. Wang, Phys. Rev. E **85**, 051142 (2012).
- ²⁷ B. K. Agarwalla, H. Li, B. Li, and J.-S. Wang, Phys. Rev. E **89**, 052101 (2014).
- ²⁸ G.-M. Tang, F. Xu, and J. Wang, Phys. Rev. B **89**, 205310 (2014).
- ²⁹ G.-M. Tang, and J. Wang, Phys. Rev. B **90**, 195422 (2014).
- ³⁰ Z. Yu, G.-M. Tang, and J. Wang, Phys. Rev. B **93**, 195419 (2016).
- ³¹ L. V. Keldysh, Zh. Eksp. Teor. Fiz. **47**, 1515 (1964) [Sov. Phys. JETP **20**, 1018 (1965)].
- ³² H. Haug, and A.-P. Jauho, *Quantum Kinetics in Transport and Optics of Semiconductors*, Springer-Verlag, Berlin (1998).
- ³³ A. Kamenev, in *Strongly Correlated Fermions and Bosons in Low-Dimensional Disordered Systems, NATO Science Series II*, Vol. 72, edited by I. V. Lerner, B. L. Altshuler, V. I. Falko, and T. Giamarchi (Kluwer, Dordrecht, 2002).
- ³⁴ A. Kamenev, 2011, *Field Theory of Non-Equilibrium Systems*, (Cambridge University Press, Cambridge, 2011).
- ³⁵ M. Campisi, P. Hänggi, and P. Talkner, Rev. Mod. Phys. **83**, 771 (2011).
- ³⁶ M. Campisi, P. Talkner, and P. Hänggi, Phys. Rev. E **83**, 041114 (2011).
- ³⁷ M. Campisi, P. Talkner, and P. Hänggi, Phys. Rev. Lett. **105**, 140601 (2010).
- ³⁸ U. Sivan and Y. Imry, Phys. Rev. B **33**, 551 (1986).
- ³⁹ M. J. Kearney and P. N. Butcher, J. Phys. C. **21**, L265 (1988).
- ⁴⁰ M. Buttiker, Phys. Rev. B **46**, 12485 (1992).
- ⁴¹ M. Ramm, T. Pruttivarasin, and H. Häffner, New J. Phys. **16**, 063062 (2014)
- ⁴² B. Sothmann, R. Sánchez, A. N. Jordan, and M. Büttiker, Phys. Rev. B **85**, 205301 (2012).
- ⁴³ I. G. Lang and Y. A. Firsov, JETP **16**, 1301 (1963)
- ⁴⁴ Z. Yu, L. Zhang, Y. Xing, and J. Wang, Phys. Rev. B **90**, 115428 (2014).
- ⁴⁵ C. Flindt, C. Fricke, F. Hohls, T. Novotný, K. Netočný, T. Brandes, and R. J. Haug, Proc. Natl. Acad. Sci. **106**, 10116 (2009).
- ⁴⁶ J. Tobiska, and Yu. V. Nazarov, Phys. Rev. B **72**, 235328 (2005).
- ⁴⁷ H. Förster, and M. Büttiker, Phys. Rev. Lett. **101**, 136805 (2008).